

AD-A159 159

NONLINEAR ANALYSIS OF A RELATIVISTIC BEAM-PLASMA
CYCLOTRON INSTABILITY(U) NAVAL RESEARCH LAB WASHINGTON
DC P SPRANGLE ET AL. 19 SEP 85 NRL-NR-5595

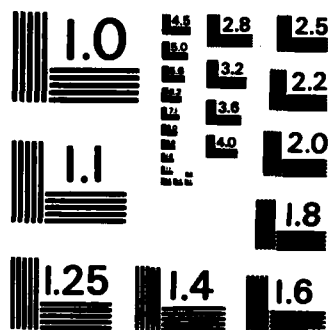
1/1

UNCLASSIFIED

F/G 20/7

NL

								END					
								FILED					
								DTIC					



MICROCOPY RESOLUTION TEST CHART
NATIONAL BUREAU OF STANDARDS-1963-A

AD-A159 159

2

NRL Memorandum Report 5595

Nonlinear Analysis of a Relativistic Beam-Plasma Cyclotron Instability

P. SPRANGLE

*Plasma Theory Branch
Plasma Physics Division*

L. VLAHOS

*Department of Physics and Astronomy
University of Maryland
College Park, MD 20742*

September 19, 1985

This work was supported by the National Aeronautics and Space Administration
and the Office of Naval Research.



NAVAL RESEARCH LABORATORY
Washington, D.C.

DTIC
ELECTE
SEP 16 1985
S D

DTIC FILE COPY

Approved for public release; distribution unlimited.

85 9 13 008

SECURITY CLASSIFICATION OF THIS PAGE

AD - A159159

REPORT DOCUMENTATION PAGE				
1a REPORT SECURITY CLASSIFICATION UNCLASSIFIED			1b RESTRICTIVE MARKINGS	
2a SECURITY CLASSIFICATION AUTHORITY			3 DISTRIBUTION / AVAILABILITY OF REPORT	
2b DECLASSIFICATION / DOWNGRADING SCHEDULE			Approved for public release; distribution unlimited.	
4 PERFORMING ORGANIZATION REPORT NUMBER(S) NRL Memorandum Report 5595			5 MONITORING ORGANIZATION REPORT NUMBER(S)	
6a. NAME OF PERFORMING ORGANIZATION Naval Research Laboratory	6b. OFFICE SYMBOL (If applicable) Code 4790	7a. NAME OF MONITORING ORGANIZATION Office of Naval Research		
6c. ADDRESS (City, State, and ZIP Code) Washington, DC 20375-5000		7b. ADDRESS (City, State, and ZIP Code) Arlington, VA 22217		
8a. NAME OF FUNDING / SPONSORING ORGANIZATION Office of Naval Research	8b. OFFICE SYMBOL (If applicable)	9. PROCUREMENT INSTRUMENT IDENTIFICATION NUMBER		
8c. ADDRESS (City, State, and ZIP Code) Arlington, VA 22217		10. SOURCE OF FUNDING NUMBERS		
		PROGRAM ELEMENT NO. 61153N	PROJECT NO.	TASK NO. RR011-09-41 WORK UNIT ACCESSION NO. DN480-639
11 TITLE (Include Security Classification) Nonlinear Analysis of a Relativistic Beam-Plasma Cyclotron Instability				
12. PERSONAL AUTHOR(S) Sprangle, P. and Vlahos, L.*				
13a. TYPE OF REPORT Interim	13b. TIME COVERED FROM 10/84 TO 9/85	14. DATE OF REPORT (Year, Month, Day) 1985 September 19	15. PAGE COUNT 36	
16 SUPPLEMENTARY NOTATION *Department of Physics and Astronomy, University of Maryland, College Park, MD 20742 (Continues)				
17 COSATI CODES			18. SUBJECT TERMS (Continue on reverse if necessary and identify by block number)	
FIELD	GROUP	SUB-GROUP	Beam plasma Relativistic Cyclotron maser	
19 ABSTRACT (Continue on reverse if necessary and identify by block number)				
<p>A self-consistent set of nonlinear and relativistic wave-particle equations are derived for a magnetized beam-plasma system interacting with electromagnetic cyclotron waves. In particular, the high frequency cyclotron mode interacting with a streaming and gyrating electron beam within a background plasma is considered in some detail. This interaction mode may possibly find application as a high power source of coherent short wavelength radiation for laboratory devices. The background plasma, although passive, plays a central role in this mechanism by modifying the dielectric properties in which the magnetized electron beam propagates. For a particular choice of the transverse beam velocity, i.e., speed of light/relativistic mass factor, the interaction frequency equals the nonrelativistic electron cyclotron frequency times the relativistic mass factor. For this choice of transverse beam velocity the detrimental effects of a longitudinal beam velocity spread is virtually removed. Power conversion efficiencies in excess of 18% are both analytically calculated and obtained through numerical simulations of the wave-particle equations. The quality of the electron beam, degree of energy and pitch angle spread, and its effect on the beam-plasma cyclotron instability is studied. <i>Keywords: Cyclotron maser.</i></p>				
20 DISTRIBUTION / AVAILABILITY OF ABSTRACT <input checked="" type="checkbox"/> UNCLASSIFIED/UNLIMITED <input type="checkbox"/> SAME AS RPT <input type="checkbox"/> DTIC USERS			21 ABSTRACT SECURITY CLASSIFICATION UNCLASSIFIED	
22a NAME OF RESPONSIBLE INDIVIDUAL P. Sprangle			22b TELEPHONE (Include Area Code) (202) 767-3493	22c. OFFICE SYMBOL Code 4790

DD FORM 1473, 84 MAR

83 APR edition may be used until exhausted

All other editions are obsolete

SECURITY CLASSIFICATION OF THIS PAGE

16. SUPPLEMENTARY NOTATION (Continued)

This work was supported by the National Aeronautics and Space Administration and the Office of Naval Research.

Accession For	
NTIS GRA&I	<input checked="" type="checkbox"/>
DTIC TAB	<input type="checkbox"/>
Unannounced	<input type="checkbox"/>
Justification	
By	
Distribution/	
Availability Codes	
Dist	Avail and/or Special
A-1	



CONTENTS

I. INTRODUCTION	1
II. PARTICLE DYNAMICS	4
III. SELF-CONSISTENT EVOLUTION OF FIELDS	6
IV. LINEAR GROWTH RATES FOR BEAM-PLASMA CYCLOTRON INTERACTIONS	10
V. EFFECTS OF VELOCITY SPREADS	15
VI. BEAM QUALITY AND VELOCITY SPREAD	17
VII. EFFICIENCY AND SATURATION OF THE HIGH FREQUENCY INTERACTION	19
VIII. NUMERICAL ILLUSTRATIONS	21
IX. DISCUSSION	22
ACKNOWLEDGMENTS	23
REFERENCES	30

NONLINEAR ANALYSIS OF A RELATIVISTIC BEAM-PLASMA CYCLOTRON INSTABILITY

I. Introduction

Electromagnetic electron cyclotron interactions have been applied to a wide range of phenomena ranging from radiation and acceleration processes in astrophysics to laboratory radiation and acceleration sources. In general an electron cyclotron instability results from a resonance between the electron's cyclotron motion with the Doppler-shifted electromagnetic wave frequency. One class of coherent electron cyclotron instabilities which relies on relativistic effects associated with the electron motion is called the electron cyclotron "maser" or "gyrotron" instability. In this instability the electron's cyclotron frequency is a function of the electron's energy (nonisochronous rotation). Under certain conditions, i.e., if the Doppler shifted radiation frequency is slightly higher than the electron cyclotron frequency, the electrons can experience azimuthal phase bunching. The resulting electron current density excites coherent radiation. This mechanism was proposed independently in the late 1950's by a number of researchers¹⁻⁴ and is the basis of the electron cyclotron maser radiation source (gyrotron)⁵⁻²⁸ and is also generally believed to be responsible for radiation observed from the earth's magnetic poles,²⁹⁻³¹ solar atmosphere³²⁻³⁴ and tandem mirror devices.^{35,36}

Under conditions of resonance, electromagnetic cyclotron waves can also result in electron acceleration. This mechanism has been proposed as a potential laser driven acceleration scheme³⁷⁻³⁹ as well as a possible mechanism responsible for the high energy electrons observed in type III solar burst.⁴⁰

In this paper we derive a set of one dimensional, fully nonlinear and relativistic wave-particle equations which describe the evolution of a system of particles in a magnetic field. Both the beam and plasma electron dynamics are treated fully nonlinearly and self-consistently and the ions are assumed infinitely massive. This formulation is used to study a beam-plasma cyclotron instability which may have applications as a source of powerful coherent, high frequency radiation. The particular cyclotron instability which we consider in some detail is the high frequency Doppler shifted interaction. This interaction has been extensively studied in the absence of a background plasma.^{22-24,38} In the absence of a plasma, the concept which utilizes a self resonance condition on the high frequency Doppler shifted interaction is referred to as the cyclotron-autoresonance maser⁴¹ (CARM). For an excellent review of this promising millimeter and submillimeter radiation mechanism, see Ref. 19. For a magnetized relativistic electron beam propagating in a low density plasma the frequency of this interaction is $\omega = \gamma \Omega_0$ where γ is the relativistic mass factor and Ω_0 is the nonrelativistic electron cyclotron frequency, and can substantially exceed the nonrelativistic electron cyclotron frequency. For MeV electron beams, magnetic fields in the tens of kG range and plasma densities of $\sim 10^{15} \text{ cm}^{-3}$, the radiation wavelength is well into the millimeter regime. For the instability to develop the electron beam must have a nonzero average transverse velocity component with respect to the magnetic field. We find that if the electron beam transverse velocity normalized to the speed of light is equal to the inverse of the relativistic mass factor, i.e., $\beta_{\perp} = 1/\gamma$, the high frequency instability can be optimized in various ways. For $\beta_{\perp} = 1/\gamma$ an autoresonance exists between the streaming and gyrating beam electrons in a background plasma and a propagating electromagnetic wave. The background plasma, although passive, plays an important role in the interaction by effectively modifying the dielectric medium in which the

electron beam propagates. Also conversion efficiencies, radiation power/beam power, can exceed 20% for practical device parameters. The dependence of beam velocity spread on the efficiency is studied. We find, for example, that if $\beta_{\perp} = 1/\gamma$ the effects of a finite axial particle velocity spread has little influence on the efficiency, however, a spread in the particle's pitch angle can significantly reduce the efficiency.

In Section II the beam-plasma particle orbit equations are derived for a right hand circularly polarized electromagnetic field. The equations describing the evolution of this field are derived in Section III. In Section IV the linear regime of the various cyclotron interactions are discussed with emphasis on the high frequency mode. Sections V and VI discuss the effects of a beam velocity spread on the instability and in Section VII an analytical expression for efficiency is obtained. The results of numerically solving the system particle-wave equations are presented in Section VIII for laboratory parameters.

II. Particle Dynamics

In this section the relativistic, nonlinear particle orbit equations are obtained in a convenient representation. These particle orbits are used in Section III to derive the appropriate driving currents for the electromagnetic field. The current densities are, in turn, used to derive a system of self-consistent, fully relativistic equations describing the temporal evolution of the wave.

The transverse vector potential associated with the right hand circularly polarized electromagnetic field is represented by

$$\underline{A}(z,t) = A(t) (\sin \phi(z,t) \hat{e}_x + \cos \phi(z,t) \hat{e}_y), \quad (1)$$

where $A(t)$ is the temporally varying amplitude of the circularly polarized wave, $\phi(z,t) = k_z z - \int_0^t \omega(t') dt'$ is the phase of $\underline{A}(z,t)$, k_z is the wave number, and $\omega(t)$ is the temporally varying frequency.

The relativistic orbit equations, for electrons in the fields given by Eq. (1) together with the axial magnetic field $\underline{B} = B_0 \hat{e}_z$, are

$$\dot{\underline{p}} = (\underline{\Omega}_0 \times \underline{p})/\gamma - |e| (-c^{-1} \partial \underline{A}/\partial t + \underline{p} \times (\nabla \times \underline{A})/\gamma m_0) \quad (2)$$

where $\underline{p} = \gamma m_0 \underline{v}$ is the particle momentum vector, $\underline{\Omega}_0 = \Omega_0 \hat{e}_z$, $\Omega_0 = |e| B_0 / m_0 c$ is the nonrelativistic electron cyclotron frequency, $\gamma = (1 + (\underline{p}/m_0 c)^2)^{1/2}$ is the Lorentz factor, m_0 is the electron's rest mass, e is the electronic charge and the dot denotes a total time derivative. Substituting (1) into (2), the three components of the momentum equation become

$$\dot{p}_x = -\frac{\Omega_0}{\gamma} p_y - \frac{|e| A(t)}{c} [(\omega(t) - v_z k_z) \cos \phi(z,t) - \Gamma(t) \sin \phi(z,t)], \quad (3a)$$

$$\dot{p}_y = \frac{\Omega_0}{\gamma} p_x + \frac{|e| A(t)}{c} [(\omega(t) - v_z k_z) \sin \phi(z, t) + \Gamma(t) \cos \phi(z, t)], \quad (3b)$$

$$\dot{p}_z = - |e| k_z \frac{A(t)}{\gamma m_0 c} [p_x \cos \phi(z, t) - p_y \sin \phi(z, t)], \quad (3c)$$

where $\Gamma(t) = A^{-1}(t) \partial A(t) / \partial t$ is the nonlinear growth or decay rate of the electromagnetic field and $v_z = p_z / \gamma m_0$. A convenient representation for the transverse particle momenta is $p_x = p_\perp \cos \theta$, and $p_y = p_\perp \sin \theta$, where $p_\perp = p_\perp(z_0, \theta_0, p_0, t)$ is the magnitude and $\theta = \theta(z_0, \theta_0, p_0, t)$ is the phase of the transverse particle momentum at time t having the initial values z_0, θ_0 and p_0 . Using the transverse momentum representation, the orbit equations in (3) become

$$\dot{p}_\perp = - \frac{|e| A}{c} [(\omega - p_z k_z / \gamma m_0) \cos \psi - \Gamma \sin \psi], \quad (4a)$$

$$\begin{aligned} \dot{\psi} = & -(\omega - p_z k_z / \gamma m_0 - \Omega_0 / \gamma) \\ & + \frac{|e| A}{c p_\perp} [(\omega - p_z k_z / \gamma m_0) \sin \psi + \Gamma \cos \psi], \end{aligned} \quad (4b)$$

$$\dot{p}_z = - \frac{|e| A k_z}{\gamma m_0 c} p_\perp \cos \psi, \quad (4c)$$

where $\psi = \theta(t) + \phi(z, t)$ is the relative phase between the particle transverse momentum and the electromagnetic wave. The rate of change of γ in this representation is

$$\dot{\gamma} = - \frac{|e| A p}{\gamma m_0^2 c^3} (\omega \cos \psi - \Gamma \sin \psi). \quad (5)$$

III. Self-Consistent Evolution of Fields

The one dimensional wave equations for the vector potential $\underline{A}(z,t)$ is

$$\left(\frac{\partial^2}{\partial z^2} - \frac{1}{c^2} \frac{\partial^2}{\partial t^2}\right) \underline{A} = \frac{-4\pi}{c} \underline{J}_\perp, \quad (6)$$

where $\underline{J}(z,t)$ is the response particle current density which will be determined by taking appropriate averages over the particle orbits. Substituting (1) into (6), the wave equation can be cast into the form

$$\alpha(t) \cos \phi(z,t) + \beta(t) \sin \phi(z,t) = -4\pi c J_x(z,t), \quad (7a)$$

$$-\alpha(t) \sin \phi(z,t) + \beta(t) \cos \phi(z,t) = -4\pi c J_y(z,t), \quad (7b)$$

where $\alpha(t) = (2\Gamma\omega + \partial\omega/\partial t)A$ and $\beta(t) = (\omega^2 - c^2 k_z^2 - \Gamma^2 - \partial\Gamma/\partial t)A$.

To obtain α and β explicitly in terms of the response current density we multiply (7a) and (7b) by $\cos \phi$ and $\sin \phi$. Upon integrating the resulting equations over z from 0 to $2\pi/k_z$ we obtain

$$\alpha(t) = -2k_z c \int_0^{2\pi/k_z} dz (J_x(z,t) \cos \phi(z,t) - J_y(z,t) \sin \phi(z,t)), \quad (8a)$$

$$\beta(t) = -2k_z c \int_0^{2\pi/k_z} dz (J_x(z,t) \sin \phi(z,t) + J_y(z,t) \cos \phi(z,t)), \quad (8b)$$

In Eqs. (8), the spatial integral is taken from 0 to $2\pi/k_z$ rather than from 0 to ∞ . The reason for this is that we are considering solutions for the fields that are spatial periodic with a period equal to a wavelength $2\pi/k_z$ and with temporally varying amplitudes and frequencies. The temporal evolution of α and β completely characterizes the electromagnetic wave. To obtain the temporal

dependence of α , and β , and hence the wave amplitude and frequency, the self-consistent current densities are needed.

The particle current density can be expressed in terms of the particle velocities averaged over the initial particle distribution function. The average current density can be shown to be given by

$$\underline{J}(z, t) = -|e|n_b \int d^3p_o \int dz_o f_o(z_o, \underline{p}_o, t=0) \underline{\tilde{v}}(z_o, \underline{p}_o, t) \delta(z - \underline{\tilde{z}}(z_o, \underline{p}_o, t)), \quad (9)$$

where n_b is the average ambient particle density, $\underline{\tilde{z}}(z_o, \underline{p}_o, t)$ and $\underline{\tilde{v}}(z_o, \underline{p}_o, t) = \underline{\tilde{p}}/\gamma m_o$ denotes the axial position and velocity of the particle with initial position z_o and initial momentum vector \underline{p}_o , $f_o(z_o, \underline{p}_o, t=0)$ is the initial Vlasov distribution function and the integrals are performed over all initial momenta and positions. The initial distribution function f_o is assumed to be spatially symmetric about the z axis and normalized such that $n_b \int f_o(z_o, \underline{p}_o, t=0) d^3p_o = n_b(z_o, t=0)$, where $n_b(z_o, t=0)$ is the initial beam particle density and $d^3p_o = p_{o\perp} dp_{o\perp} dp_{oz} d\theta_o$. In obtaining the current density representation in (9) the actual particle distribution function was written as a sum of the individual particle distribution function. For a large number of particles the sum can be replaced by integrals over the initial momentum and position of the particles. Generalizing the response current in (9) to more than one particle species evolves summing (9) over the various particle distributions. Substituting (9) into Eqs. (8) together with the representation for the transverse momentum, and performing the specified integration over z yields

$$\left(\frac{\alpha(t)}{\beta(t)} \right) = \frac{4\pi |e| n_b c}{m_0} \left[2\pi \iint p_{o\perp} dp_{o\perp} dp_{oz} g_o(p_{o\perp}, p_{oz}) \left\langle \frac{p_{\perp}}{\gamma} \left(\frac{\cos \psi}{\sin \psi} \right) \right\rangle_{\psi_o} \right], \quad (10)$$

where $\psi = \psi(z_o, p_o, t)$, the average is defined as $\langle \dots \rangle_{\psi_o} = \frac{1}{2\pi} \int_0^{2\pi} d\psi_o$, $\psi_o = \phi_o + \theta_o$ and $g_o(p_{o\perp}, p_{oz}) = f_o(z_o, p_o, t=0)$ is the initial distribution function which is assumed to be axially symmetric and spatially homogeneous.

The initial Vlasov distribution is normalized such that

$2\pi \iint p_{o\perp} dp_{o\perp} dp_{oz} g_o(p_{o\perp}, p_{oz}) = 1$. In obtaining (10) we used that relationship $\int_0^{2\pi/k_z} dz_o = \int_0^{2\pi} d\psi_o$. In general the integration over z_o in Eqs. (10) should include all initial particle positions. However, in Eqs. (8) the integration over z extends from 0 to $2\pi/k_z$ and since the system of particles and fields are periodic in z , we may take the z_o integration range in (10) to be from 0 to $2\pi/k_z$.

Normalized Particle-Wave Equations

The expressions in (10) together with the orbit equations in (4) describe the fully nonlinear evolution of the fields represented by (1). Introducing normalized variables, the orbit equations in (4) become

$$\frac{\partial u_{\perp}}{\partial \tau} = -a \left[\left(\bar{\omega} - \frac{u_z \bar{k}_z}{\gamma} \right) \cos \psi - \bar{\Gamma} \sin \psi \right], \quad (11a)$$

$$\frac{\partial \psi}{\partial \tau} = -\Delta \bar{\Omega} + \frac{a}{u_{\perp}} \left[\left(\bar{\omega} - \frac{u_z \bar{k}_z}{\gamma} \right) \sin \psi + \bar{\Gamma} \cos \psi \right], \quad (11b)$$

$$\frac{\partial u_z}{\partial \tau} = -a \bar{k}_z \frac{u_{\perp}}{\gamma} \cos \psi, \quad (11c)$$

and the field equations in (10) become

$$(2\bar{\Gamma}\bar{\omega} + \frac{\partial\bar{\omega}}{\partial\tau})a = \bar{\omega}_b^2 [2\pi \iint p_{o\perp} dp_{o\perp} dp_{oz} g_o < \frac{u_{\perp}}{\gamma} \cos \psi >_{\psi_o}], \quad (12a)$$

$$(\bar{\omega}^2 - \bar{k}_z^2 - \bar{k}_{\perp}^2 - \bar{\Gamma}^2 - \frac{\partial\bar{\Gamma}}{\partial\tau})a = \bar{\omega}_b^2 [2\pi \iint p_{o\perp} dp_{o\perp} dp_{oz} g_o < \frac{u_{\perp}}{\gamma} \sin \psi >_{\psi_o}], \quad (12b)$$

where $u_{\perp} = p_{\perp}/m_o c$, $u_z = p_z/m_o c$, $\tau = \Omega_o t / \langle \gamma_o \rangle$, $\langle \gamma_o \rangle$ is the average initial value of γ , $a = |e| A/m_o c^2$, $\bar{\omega} = \omega/(\Omega_o / \langle \gamma_o \rangle)$, $\bar{k}_z = ck_z/(\Omega_o / \langle \gamma_o \rangle)$, $\bar{k}_{\perp} = ck_{\perp}/(\Omega_o / \langle \gamma_o \rangle)$, $\bar{\Gamma} = \Gamma/(\Omega_o / \langle \gamma_o \rangle)$, $\Delta\bar{\omega} = \bar{\omega} - u_z \bar{k}_z / \gamma - \langle \gamma_o \rangle / \gamma$, $\bar{\omega}_b = \omega_b/(\Omega_o / \langle \gamma_o \rangle)$ and $\omega_b = (4\pi |e|^2 n_b / m_o)$ is the plasma frequency. For completeness we include the normalized form of (7)

$$\frac{d\gamma}{d\tau} = - \frac{u_{\perp}}{\gamma} a (\bar{\omega} \cos \psi - \bar{\Gamma} \sin \psi). \quad (13)$$

The initial conditions for Eqs. (11), (12) and (13) are $u_{\perp}(\tau=0) = u_{o\perp}$, $u_z(\tau=0) = u_{oz}$, $\gamma(\tau=0) = \gamma_o$, $\psi(\tau=0) = \psi_o$, $\bar{\omega}(\tau=0) = \bar{\omega}_o$ and $\bar{\Gamma}(\tau=0) = 0$.

Up to this point we have considered a general distribution of particles interacting nonlinearly with electromagnetic and electrostatic waves. The present formulation can treat several particle species such as a beam and background plasma by simply taking the initial Vlasov distribution function $g_o(p_{o\perp}, p_{oz})$ to be a sum over all the particle species. In this approach all the particle species are treated fully nonlinearly and self-consistently.

IV. Linear Growth Rates for Beam-Plasma Cyclotron Interactions

The linear electromagnetic dispersion relation, in unnormalized units, for a cold magnetized electron beam propagating and gyrating within a cold stationary plasma can be derived from the fully nonlinear equations in (11) and (12). The details of the derivation will not be given here, but can be found in Ref. (34). The electromagnetic dispersion relation is

$$\omega^2 - c^2 k_z^2 - \frac{\omega_p^2 \omega}{\omega - \Omega_0} = \frac{\omega_b^2}{\gamma_0} \left[\frac{\omega - v_{0z} k_z}{\omega - v_{0z} k_z - \Omega_0 / \gamma_0} - \frac{\beta_{0\perp}^2 (\omega^2 - c^2 k_z^2)}{2 (\omega - v_{0z} k_z - \Omega_0 / \gamma_0)^2} \right]. \quad (14)$$

The left-hand side of (14) represents the electromagnetic dispersion relation for right-hand circularly polarized waves in a cold, stationary plasma with plasma frequency ω_p . The right-hand side of (14) represents the coupling term due to the propagating and gyrating beam. The beam is taken to have a plasma frequency ω_b , axial velocity v_{0z} and transverse velocity $v_{0\perp} = c\beta_{0\perp}$.

In general there are three unstable interaction frequencies associated with the dispersion relation. Figure 1 shows the general features of the dispersion relation and the three possible intersection frequencies for waves propagating along the magnetic field. In this section we will be primarily concerned with finding the linear growth rates for the medium and high frequency modes, labeled ω_1 and ω_2 , respectively. To solve for the growth rates we set $\omega = \omega_0 + \delta\omega$, where $\omega_0 = v_{0z} k_z + \Omega_0 / \gamma_0$ and is the Doppler shifted cyclotron frequency and $|\omega_0| \gg |\delta\omega|$. The dispersion relation reduces to

$$\begin{aligned}
2\omega_0 \left[1 + \frac{\omega_p^2 \Omega_0 / \omega_0}{2(\omega_0 - \Omega_0)(\omega_0 - \Omega_0 + \delta\omega)} \right] \delta\omega \\
= \frac{\omega_b^2}{\gamma_0} \left[\frac{\Omega_0 / \gamma_0}{\delta\omega} - \frac{\beta_{0\perp}^2}{2} \frac{(\omega_0^2 - c^2 k_z^2 + 2\omega_0 \delta\omega)}{\delta\omega^2} \right], \quad (15)
\end{aligned}$$

where we have set $\omega - v_z k_z$ equal to Ω_0 / γ_0 on the right-hand side of (14) and have taken the Doppler shifted cyclotron frequency ω_0 to lie on the electromagnetic dispersion curve, hence ω_0 satisfies $\omega_0^2 - c^2 k_z^2 - \omega_p^2 \omega_0 / (\omega_0 - \Omega_0) = 0$.

Case 1 (medium frequency interaction, $\omega = \omega_1 \geq \Omega_0$)

In the absence of the beam, $\omega_b = 0$, the frequency of the electromagnetic wave in the background magnetized plasma, for waves slightly above the cut-off frequency, is given by

$$\omega_0 = \omega_{co} \left(1 + \frac{\omega_p^2}{\omega_{co}^2} \frac{c^2 k_z^2}{\omega_{co}^2 + \omega_p^2} \right), \quad (16)$$

where $\omega_{co} = \Omega_0 (1 + \omega_p^2 / \Omega_0^2)$ is the cut-off frequency, $|ck_z| < \omega_{co}$ and we have assumed $\omega_p \ll \Omega_0$.

In this limit the dispersion relation in (15) reduces to

$$\left(\frac{\Omega_0^3}{\Omega_0 \delta\omega + \omega_p^2} \right) \delta\omega = \frac{\omega_b^2}{\gamma_0} \left[\frac{\Omega_0 / \gamma_0 - \beta_{0\perp}^2 \Omega_0}{\delta\omega} - \frac{\beta_{0\perp}^2}{2} \frac{\Omega_0^2}{\delta\omega^2} \right], \quad (17)$$

where $\delta\omega = \omega - \omega_0$ and ω_0 is given by (16). Assuming that $|\delta\omega| \ll \gamma_0 \beta_{0\perp}^2 \Omega_0 / 2$ we find that

$$\delta\omega^3 = - \frac{\omega_b^2 \beta_{o\perp}^2}{2\gamma_o \Omega_o} (\omega_p^2 + \Omega_o \delta\omega). \quad (18)$$

From (18) we find that the growth rate for a wave propagating along the magnetic field with a frequency near the cut-off frequency,

$$\omega_{co} = \Omega_o (1 + \omega_p^2/\Omega_o^2) = \Omega_o, \text{ is}$$

$$\Gamma = \text{Im}(\delta\omega) = \frac{\sqrt{3}}{2} \left(\frac{1}{2} \frac{\omega_p^2}{\Omega_o} \frac{\omega_b^2}{\gamma_o} \beta_{o\perp}^2 \right)^{1/3}, \quad (19a)$$

for $\Gamma \ll \omega_p^2/\Omega_o$ or

$$\Gamma = \omega_b \beta_{o\perp} / \sqrt{2\gamma_o}, \quad (19b)$$

for $\Gamma \gg \omega_p^2/\Omega_o$.

This result should be compared to the usual growth rate associated with the cyclotron maser instability. That is, taking $\omega_p = 0$, $k_z = 0$ and introducing a transverse wave number k_\perp , it can be shown that the usual cyclotron maser growth rate is

$$\Gamma_{\text{maser}} = \frac{\sqrt{3}}{2} \left(\frac{ck_\perp}{2} \frac{\omega_b^2}{\gamma_o} \beta_{o\perp}^2 \right)^{1/3}. \quad (20)$$

Comparing (19a) with (20) we note that the effect of the background plasma is equivalent to an effective transverse wave number. The effective transverse wave number introduced by the background plasma is not, however, ω_{co}/c , as would be expected, but is substantially smaller, due to the presence of the nearby cyclotron mode, and equal to $(\omega_p^2/\omega_{co}^2)\omega_{co}/c = \omega_p^2/(\Omega_o c)$.

Case 2 (high frequency interaction, $\omega = \omega_2 \gg \Omega_0$)

For the case where $\omega_2 \gg \Omega_0$ we find that $\omega_0 = (c^2 k_z^2 + \omega_p^2)^{1/2} = ck_z (1 + \omega_p^2 / (2c^2 k_z^2))$, where $\omega_0 \gg \Omega_0 \gg \omega_p$. Hence the dispersion relation in (15) reduces to

$$\delta\omega^3 = \frac{-\omega_b^2}{2\omega_0 \gamma_0} \left[\frac{\beta_{0\perp}^2}{2} \omega_p^2 - \left(\frac{\Omega_0}{\gamma_0} - \beta_{0\perp}^2 \omega_0 \right) \delta\omega \right]. \quad (21)$$

Since $\omega_0 = v_z k_z + \Omega_0 / \gamma_0 = (c^2 k_z^2 + \omega_p^2)^{1/2}$ the wave number for this interaction is given by

$$ck_z = \frac{\Omega_0}{\gamma_0} \gamma_{oz}^2 \beta_{oz}^2 \left(1 + \left(1 - \omega_p^2 \gamma_0^2 / (\Omega_0^2 \gamma_{oz}^2) \right)^{1/2} / \beta_{oz} \right) \quad (22)$$

where $\gamma_{oz} = (1 - \beta_{oz}^2)^{-1/2}$ and $\beta_{oz} = v_{oz} / c$. Using (22) we find that the interaction frequency ω_0 is

$$\omega_0 = \frac{\Omega_0}{\gamma_0} \left[1 + \gamma_{oz}^2 \beta_{oz}^2 (\beta_{oz} + (1 - \omega_p^2 \gamma_0^2 / (\Omega_0^2 \gamma_{oz}^2))^{1/2}) \right]. \quad (23)$$

For a highly relativistic electron beam in a tenuous plasma, i.e., $\gamma_{oz} \gg 1$ and $\omega_p \gamma_0 / (\Omega_0 \gamma_{oz}) \ll 1$, the interaction frequency is $2\gamma_{oz}^2$ times higher than the relativistic cyclotron frequency, that is, $\omega_0 = 2\gamma_{oz}^2 \Omega_0 / \gamma_0 = 2\gamma_0 \Omega_0 / (1 + \gamma_0^2 \beta_{0\perp}^2)$. Two particularly simple limiting cases for the high frequency interaction can be considered.

Case 2a ($|\delta\omega| \gg \omega_p^2 \beta_{0\perp}^2 / 2|\Omega_0 / \gamma_0 - \beta_{0\perp}^2 \omega_0|$)

In this limit the dispersion relation, for a highly relativistic beam in a tenuous plasma, reduces to $\delta\omega^2 = \omega_b^2 (1 - \beta_{oz} - \beta_{0\perp}^2) / 2\gamma_0$ where

$\omega_o = 2\gamma_{oz}^2 \Omega_o/\gamma_o$. This high frequency interaction is unstable if $\beta_{o\perp}^2 + \beta_{oz} > 1$ and the growth rate is given by

$$\Gamma = \frac{\omega_b}{\sqrt{2}\gamma_o} (\beta_{o\perp}^2 + \beta_{oz} - 1)^{1/2}. \quad (24)$$

Note that (24) is valid for wave frequencies satisfying (23), no frequency mismatch. For a more complete description of the linear theory in this limit see Ref. (15).

Case 2b ($|\delta\omega| \ll \omega_p^2 \beta_{o\perp}^2 / 2|\Omega_o/\gamma_o - \beta_{o\perp}^2 \omega_o|$)

In this limit the dispersion relation in (21) reduces to

$$\delta\omega^3 = - \frac{\omega_b^2/\gamma_o}{4\omega_o} \beta_{o\perp}^2 \omega_p^2, \quad (25)$$

The linear growth rate associated with this high frequency mode is

$$\Gamma = \frac{\sqrt{3}}{2} \left(\frac{\omega_p^2}{4\omega_o} \frac{\omega_b^2}{\gamma_o} \beta_{o\perp}^2 \right)^{1/3}. \quad (26)$$

In this section the linear regime associated with the beam-plasma cyclotron interaction has been briefly discussed for the medium and high frequency interaction. The remainder of this article will deal primarily with the effects of beam velocity spreads and saturation efficiency of the high frequency interaction.

V. Effects of Velocity Spreads

A somewhat simplified but useful way of considering the role played by a beam energy spread is to examine the cyclotron resonance denominator term, $\Omega = \omega - v_{oz}k_z - \Omega_0/\gamma_0$ in the linear dispersion relation. For a beam with zero energy spread in both the longitudinal and transverse directions the resonant denominator in the linear interaction regime is nonzero and equal to the linear frequency shift $\Delta\omega_L$, that is $\Omega(v_{oz}, v_{o\perp}) = \omega - v_{oz}k_z - \Omega_0/\gamma_0 = \Delta\omega_L$, where $|\Delta\omega_L| \ll \omega$. If the beam electrons have a spread in longitudinal and transverse velocities denoted by Δv_z and Δv_\perp respectively, the cyclotron resonance term will in turn have a spread, $\Delta\Omega$. If $|\Delta\Omega|$ is small compared to the magnitude of the linear frequency shift, $|\Delta\omega_L|$, the interaction will evolve as if Δv_z and Δv_\perp were zero. If on the other hand $|\Delta\Omega|$ is large compared to $|\Delta\omega_L|$, the effect on the instability of the finite Δv_z and Δv_\perp will be significant. These simple physical arguments can be quantified by expanding $\Omega(v_z, v_\perp)$ about $v_{oz}, v_{o\perp}$, where $v_z = v_{oz} + \Delta v_z$ and $v_\perp = v_{o\perp} + \Delta v_\perp$. Expanding Ω gives $\Omega(v_z, v_\perp) = \Omega(v_{oz}, v_{o\perp}) + \Delta\Omega$, where $\Delta\Omega = (\partial\Omega/\partial v_z)\Delta v_z + (\partial\Omega/\partial v_\perp)\Delta v_\perp$, $\partial\Omega/\partial v_z = -k_z + (\Omega_0/\gamma^2)\partial\gamma/\partial v_z = -k_z + \gamma\Omega_0 v_z/c^2$ and $\partial\Omega/\partial v_\perp = (\Omega_0/\gamma^2)\partial\gamma/\partial v_\perp = \gamma\Omega_0 v_\perp/c^2$. The spread in the cyclotron resonant term due to velocity spread is therefore $\Delta\Omega = (-ck_z + \gamma_0\Omega_0\beta_{oz} + \gamma_0\Omega_0\beta_{o\perp}\alpha)\Delta v_z/c$, where $\alpha = \Delta v_\perp/\Delta v_z$. The effects of velocity spread on the evolution of the instability can be neglected if

$$|ck_z - \gamma_0\Omega_0(\beta_{oz} + \beta_{o\perp}\alpha)|\Delta v_z/c \ll |\Delta\omega_L|. \quad (27)$$

The effects of a longitudinal velocity spread can be removed to lowest order if $\gamma_0\Omega_0\beta_{oz} = ck_z$. For $\gamma_0\Omega_0\beta_{oz} = ck_z$ condition (27) becomes

$$|\Delta v_{\perp}|/c \ll \frac{|\Delta \omega_L|}{\gamma_o \beta_{o\perp} \Omega_o}. \quad (28)$$

The spread in the relativistic mass factor, γ , associated with the velocity spread is $\Delta\gamma = \gamma - \gamma_o = \gamma_o^3 (\beta_{oz} \Delta v_z + \beta_{o\perp} \Delta v_{\perp})/c$.

For a particular choice of parameters an interesting possibility arises for significantly relaxing the effects of a longitudinal beam velocity spread on the instability. If we consider the high frequency interaction regime (Case 2) for a highly relativistic electron beam in a tenuous plasma the interaction frequency is given by $\omega_o = ck_z = 2\gamma_{oz}^2 \Omega_o/\gamma_o$. Using (23) and the condition $\gamma_o \Omega_o \beta_{oz} = ck_z = \omega_o$ we find the necessary value of $\beta_{o\perp}$ required to remove the effects of a longitudinal velocity spread on the high frequency mode is $\beta_{o\perp} = 1/\gamma_o$. Taking $\beta_{o\perp} = 1/\gamma_o$, the transverse velocity spread condition in (28) becomes

$$\frac{\Delta v_{\perp}}{c} \ll \frac{|\Delta \omega_L|}{\Omega_o}. \quad (29)$$

Note that for $\beta_{o\perp} = 1/\gamma_o$ the interaction frequency is $\omega_o = \gamma_o \Omega_o$ and the condition for Case 2b (see Eq. (25)) is automatically satisfied since $\Omega_o/\gamma_o - \beta_{o\perp}^2 \omega_o$ vanishes.

VI. Beam Quality and Velocity Spread

The measure of quality of a spatially uniform electron beam propagating along and gyrating about a uniform magnetic field is given by two independent quantities. In this paper we will choose these two independent quantities to be the fractional half-width spread in the relativistic mass factor γ and the velocity pitch angle θ_0 where $\theta_0 = \beta_{0\perp}/\beta_{0z}$. That is, the measure of beam quality is determined by $\Delta\gamma/\gamma_0$ and $\Delta\theta/\theta_0$ where $\Delta\gamma/\gamma_0$ and $\Delta\theta/\theta_0$ are positive and assumed small compared to unity. Figure 2 shows the velocity distribution for a beam having a $\Delta\theta$ and $\Delta\gamma$ spread. In Fig. 2 the beam electrons are assumed to uniformly fill the crossed region. The full spread in β_z and β_{\perp} , about the average values β_{0z} and $\beta_{0\perp}$, is respectively $2\Delta\beta_z$ and $2\Delta\beta_{\perp}$. Using the symbol δ to denote the variation in a quantity from its average value, we find for individual electrons that $\delta\beta_{\perp} = \theta_0\delta\beta + \delta\theta = \theta_0(\delta\gamma/\gamma_0 + \gamma_0^2\delta\theta/\theta_0)/\gamma_0^2$ and $\delta\beta_z = \delta\beta - \theta_0\delta\theta = (\delta\gamma/\gamma_0 - \gamma_0^2\delta\theta/\theta_0)/\gamma_0^2$ where $\delta\beta = \delta\gamma/\gamma_0^3$ is the variation in the total electron's velocity and $\gamma_0 \gg 1$. Note that the variations $\delta\beta_{\perp}$, $\delta\beta_z$, $\delta\beta$, $\delta\theta$ and $\delta\gamma$ can be of either sign. For $\beta_{0\perp} = 1/\gamma_0$ and $\gamma_0 \gg 1$ the average pitch angle is $\theta_0 = 1/\gamma_0$ and the beam's half-width spread in β_{\perp} and β_z is given by

$$\Delta\beta_{\perp} = \left(\frac{\Delta\gamma}{\gamma_0} + \gamma_0^2 \frac{\Delta\theta}{\theta_0}\right)/\gamma_0^3 > 0, \quad (30a)$$

$$\Delta\beta_z = \left(\frac{\Delta\gamma}{\gamma_0} - \frac{\Delta\theta}{\theta_0}\right)/\gamma_0^2 > 0. \quad (30b)$$

The expressions in (30) give the half-width spread in the transverse and longitudinal velocities in terms of $\Delta\gamma/\gamma_0 \ll 1$ and $\Delta\theta/\theta_0 \ll 1$ for $\gamma_0 \gg 1$. Combining (30) and (29) we find that the fractional half-width spreads $\Delta\gamma/\gamma_0$ and $\Delta\theta/\theta_0$ can be neglected in the high frequency radiation excitation process

if

$$\frac{\Delta Y}{Y_0} + \gamma_0^2 \frac{\Delta \theta}{\theta_0} \ll \gamma_0^3 \frac{|\Delta \omega_L|}{\Omega_0}. \quad (31)$$

Substituting the linear frequency shift $\Delta \omega_L = (\omega_p^2 \omega_b^2 \beta_{o\perp}^2 / (4\omega_0 \gamma_0))^{1/3/2}$ i.e., the real part of $\delta \omega$ in the solution of (25), into (31) gives for the quality requirements on the electron beam

$$\frac{\Delta Y}{Y_0} + \gamma_0^2 \frac{\Delta \theta}{\theta_0} \ll \gamma_0 \left(\frac{\gamma_0 \omega_p \omega_b}{2\Omega_0^2} \right)^{2/3}, \quad (32)$$

where we have set $\beta_{o\perp} = 1/\gamma_0$ and $\omega_0 = \gamma_0 \Omega_0$. The inequality in (31) shows that a beam pitch angle spread is more detrimental to the wave-particle interaction than a beam energy spread for relativistic electron beams. This point will be demonstrated in Section VIII.

VII. Efficiency and Saturation of the High Frequency Interaction

A similar line of reasoning as used to determine estimates of velocity spread effects can be used to estimate saturation efficiencies. If electron trapping is responsible for saturating the instability one expects, for a beam without an initial velocity spread, that at saturation the resonance term becomes $\Omega(v_{sz}, v_{s\perp}) = \omega - v_{sz}k_z - \Omega_0/\gamma_s = -f \Delta\omega_L$, where v_{sz} and γ_s is the axial beam velocity and relativistic mass factor at saturation and $0 < f < 1$ is a phenomenological factor related to the fraction of trapped beam electrons in the cyclotron wave.

We now expand $\Omega(v_{sz}, v_{s\perp})$ about its initial value giving

$$\Omega(v_{sz}, v_{s\perp}) = \Omega(v_{oz}, v_{o\perp}) + (\gamma_s - \gamma_o) \frac{\partial \Omega(v_{oz}, v_{o\perp})}{\partial \gamma_o}, \quad (33)$$

where

$$\frac{\partial \Omega(v_{oz}, v_{o\perp})}{\partial \gamma_o} = \frac{\omega^2 - c^2 k_z^2}{\omega \gamma_o} = \frac{\omega_p^2}{\omega \gamma_o} = \frac{\omega_p^2 / \Omega_o}{\gamma_o^2}, \quad (34)$$

and $\Omega(v_{oz}, v_{o\perp}) = \omega - v_{oz}k_z - \Omega_o/\gamma_o = \Delta\omega_L$. In obtaining (34), the relation $d\gamma/dp_z = (\omega/k_z)m_0c^2$ was used, this relationship can be obtained from the orbit equations in (4) and (5). From (33), together with $\Omega(v_{oz}, v_{o\perp}) = \Delta\omega_L$, we find that $\gamma_o - \gamma_s = \gamma_o^2(1+f) \Delta\omega_L \Omega_o / \omega_p^2$ where $\Delta\omega_L$ is the linear frequency shift given by the $\text{Re}(\delta\omega)$ in (25). Defining the saturation efficiency as $\eta_s = (\gamma_o - \gamma_s)/(\gamma_o - 1)$, we find for $\gamma_o \gg 1$ that

$$\eta_s = \gamma_o(1+f) \frac{\Delta\omega_L \Omega_o}{\omega_p^2} = \frac{(1+f)}{2} \left(\frac{\omega_b \Omega_o}{2\omega_p^2} \right)^{2/3} \gamma_o^{-1/3}. \quad (35)$$

The approximate efficiency expression in (35) is appropriate for the case where $\beta_{o\perp} = 1/\gamma_o$, i.e., and therefore is invalid for very large and very small values of ω_p as stated in Section IV under Case 2. The efficiency expression in (35) scales as $1/\gamma_o^{1/3}$ or as the cube root of the radiation wavelength. A comparison of (35) with the numerically computed efficiencies is given in Section VIII.

VIII. Numerical Illustrations

In this article we are interested in the possibility of applying the high frequency interaction process to the generation of high power millimeter and submillimeter radiation. To this end the coupled wave particle equations in (11) and (12) are integrated numerically for the high frequency interaction which occurs at $\omega = \gamma_0^2(\Omega_0/\gamma_0)$. Typically a few hundred particles per wavelength are integrated for both the beam and plasma particles. Note that in our formulation of the problem only the dynamics of those particles in a single wavelength are needed.

Figure 3 shows the efficiency and growth rate as a function of normalized background plasma frequency for a 1.5 MeV ($\gamma_0 = 4$) and 3.5 MeV ($\gamma_0 = 8$) electron beam. The transverse beam electron velocity is $\beta_{0\perp} = 1/\gamma_0 = 0.25$, 0.125 and the beam plasma frequency is $\omega_b = 0.025 \Omega_0$. For an external magnetic field of $B_0 = 40$ kG, the beam current flux is approximately 500 A/cm². The interaction frequency is $\omega = \gamma_0 \Omega_0$, corresponding to a wavelength of $\lambda = 0.67$ mm for $\gamma_0 = 4$ and $\lambda = 0.34$ mm for $\gamma_0 = 8$. The efficiency in Fig. 3 reaches a maximum value of $\sim 18\%$ at a plasma frequency of $\omega_p = 0.2 \Omega_0$ ($n_p = 2 \times 10^{15}$ cm⁻³). The calculated saturation efficiency given in Eq. (35) for these parameters is found to be $\eta_s = 14(1+f)\%$ where f is between 0 and 1, and is in reasonable agreement with the numerical efficiency of 18%. The growth rate, at maximum efficiency for $\gamma_0 = 4$ is $\Gamma = 2 \times 10^{-3} \Omega_0/c = 4.7 \times 10^{-2}$ cm⁻¹ which corresponds to an e-folding length of $L_e = 1/\Gamma = 22$ cm.

Figure 4 shows the effect on efficiency for a beam with energy spread, $\Delta\gamma/\gamma$ and pitch angle spread $\Delta\theta/\theta_0$. The other parameters for this figure are $\beta_{0\perp} = 1/\gamma_0$, $\omega_p = 0.2 \Omega_0$ and $\omega_b = 0.025 \Omega_0$.

In Fig. 5 the saturation efficiency is shown as a function of beam energy. In this figure the transverse beam electron velocity is $\beta_{0\perp} = 1/\gamma_0$ while the beam density (current flux) and background plasma density are the same as for Fig. 4. A noteworthy feature in the figure is the relatively slow falloff in efficiency with increasing beam energy. The wavelength of the excited wave is 0.67 mm for $\gamma_0 = 4$ and 84 μm for $\gamma_0 = 32$.

IX. Discussion

We have analyzed a beam plasma cyclotron wave instability which may have application as a high efficiency, high frequency radiation source. Although our analysis is somewhat general we have concentrated on the high frequency Doppler-shifted interaction since efficient, high frequency sources are more challenging to develop. The nonlinear coupled wave particle equations were numerical solved and various plots of the radiation efficiency as a function of background plasma frequency, beam energy spread and beam particle pitch angle spread are presented. The conversion efficiency in the high frequency plasma maser source could be enhanced by appropriately contouring the external magnetic field as a function of axial position.^{16,18} Spatially contouring the external magnetic field in order to enhance efficiency has been successfully employed in conventional maser (gyrotron) devices.¹⁷

By choosing the average transverse beam velocity, $v_{0\perp}$, equal to c/γ_0 the detrimental effects of a spread in the axial beam velocity Δv_z can, to lowest order, be removed. We have shown that high efficiencies, tens of percent, can be achieved even for electron beams with large $\Delta\gamma/\gamma_0$ spreads and modest $\Delta\theta/\theta_0$ spreads, see Fig. 4. Both analytical and numerical results show that the saturation efficiency falls off gradually as the beam energy is increased, see Fig. 5.

Although not contained in the present paper our analysis shows that the present radiation mechanism may be more applicable to an oscillator configuration. The high frequency Doppler-shifted mode the background plasma merely serves to modify the index of refraction of the electromagnetic wave, making it less than unity. In principle, the background plasma can be removed and replaced by a propagating wave having a transverse spatial gradient such as waves in an open resonator configuration. An open resonator configuration has a number of important characteristics and advantages over a closed resonator or waveguide configuration.

In an open resonator transverse mode selection is a natural consequence of the larger diffraction angles associated with higher order transverse modes. Higher order transverse modes tend to propagate out of the resonator and thus have lower Q s. Longitudinal mode selection can be achieved by using a Fabry-Perot interferometer. Furthermore, since the surface area of the mirrors can be made large, open resonators can operate at extremely high power levels.

A possible configuration for a plasma cyclotron maser oscillator utilizing an open resonator cavity is shown in Fig. 6. Radiation which builds up within the resonator is extracted through a small opening in the right mirror.

Acknowledgments

This work was supported by NASA Grant NAGW-81 and ONR. Discussions with K. Papadopoulos, C. Kapetanakis and W. Manheimer were very useful.

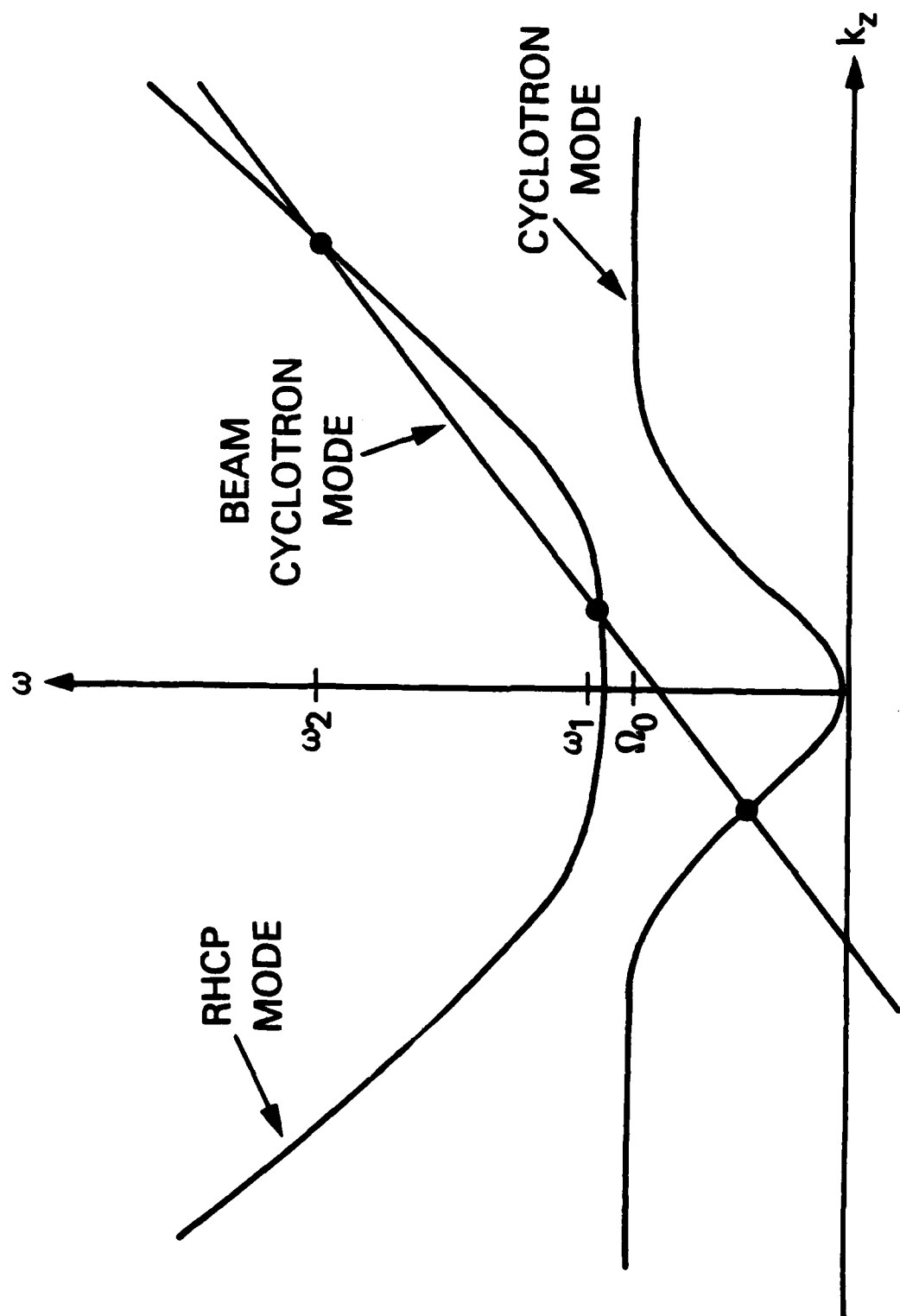


Figure 1 Shows the general features of the dispersion curve and in particular the medium, ω_1 , and high frequency, ω_2 , interaction regimes.

ELECTRON BEAM DISTRIBUTION

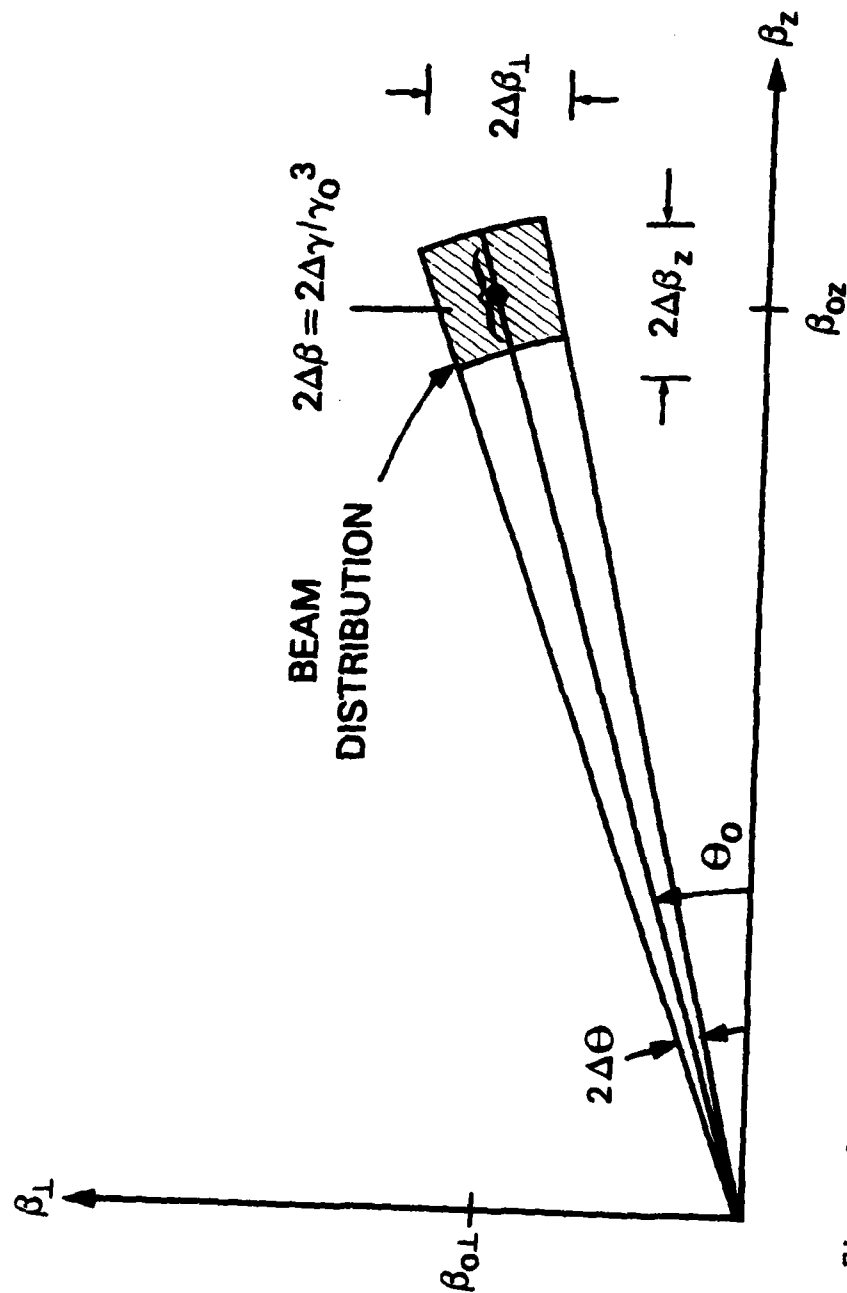


Figure 2 Shows the relationships between the half width velocity spreads $\Delta v_z = c\Delta\beta_z$ and $\Delta v_{\perp} = c\Delta\beta_{\perp}$, of an idealized beam, and the half width spreads in pitch angle and energy, $\Delta\theta$, $\Delta\gamma$.

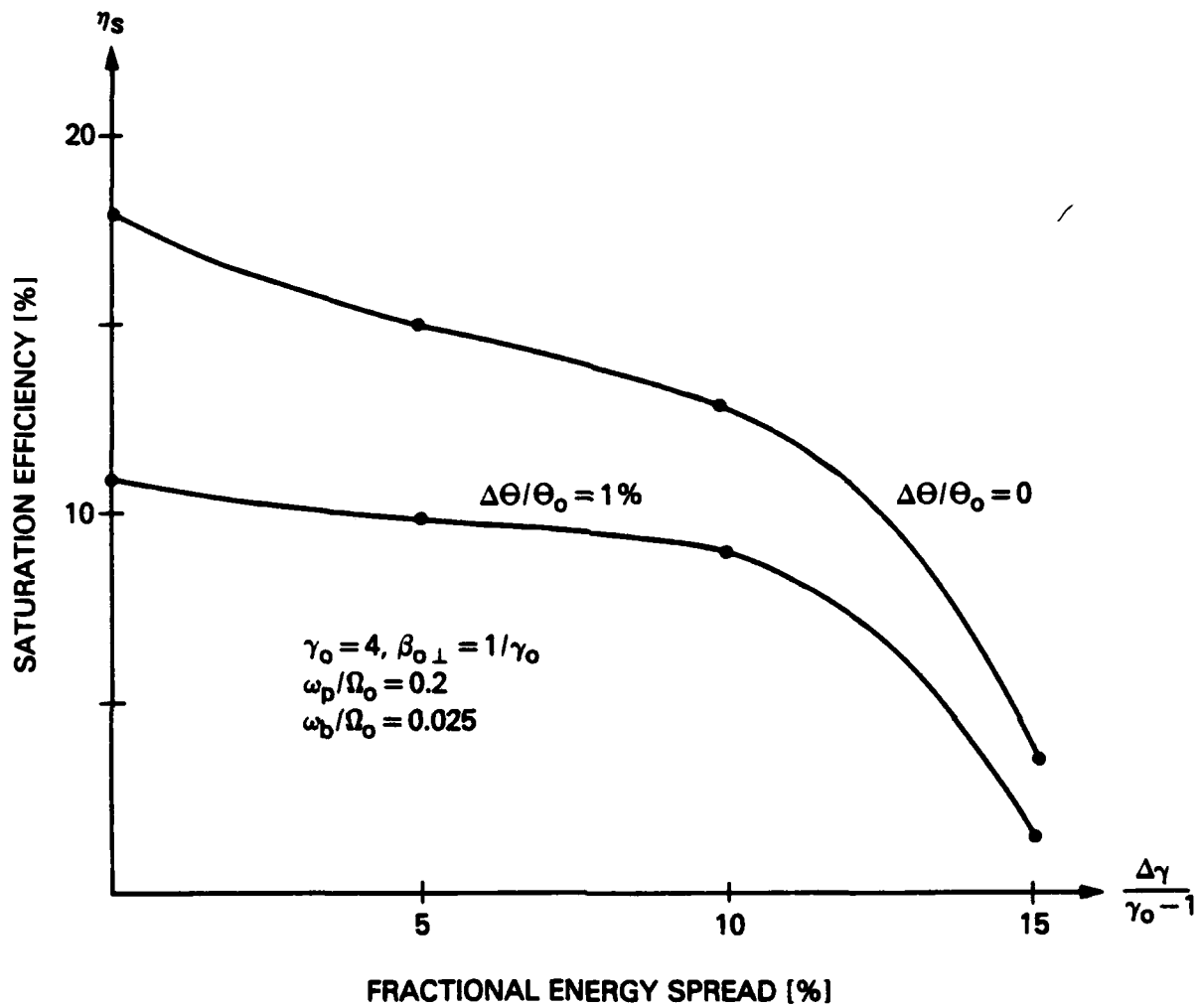


Figure 4 Shows the effect on efficiency for a beam with a half width energy spread $\Delta\gamma/\gamma_0$ and half width pitch angle spread $\Delta\theta/\theta_0$ for a beam with $\gamma_0 = 4$. Other parameters used for this figure are $\beta_{0\perp} = 1/\gamma_0$, $\omega_p = 0.2 \Omega_0$ and $\omega_b = 0.025 \Omega_0$.

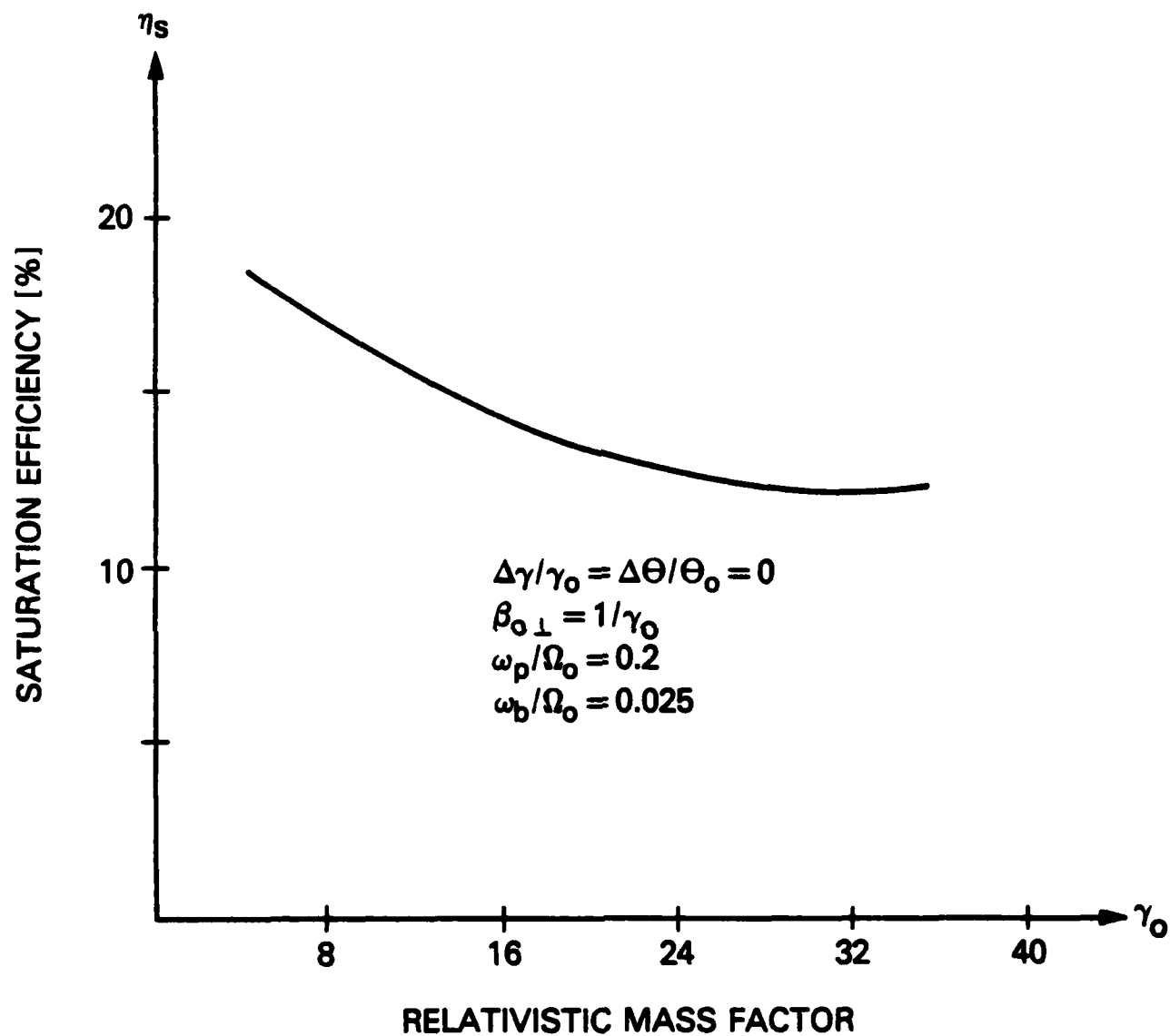


Figure 5 Shows the saturation efficiency as a function of beam energy, γ_0 .

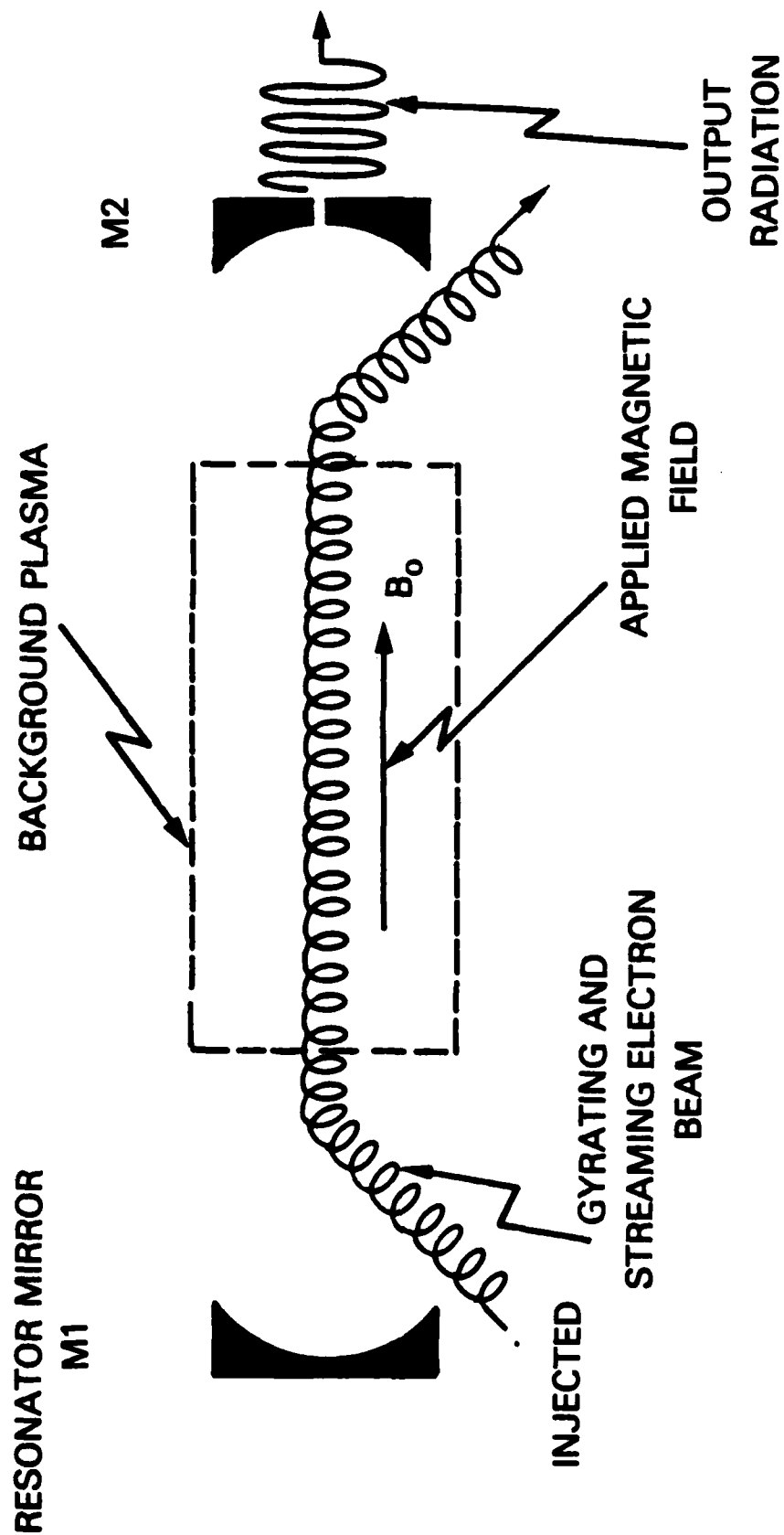


Figure 6 Shows a possible configuration for a plasma cyclotron maser oscillator source.

REFERENCES

1. R. Q. Twiss, Aust. J. Phys., 11, 564, (1958).
2. A. V. Gaponov, Isv. Vyssh. Uchebn. Zaved, Radiofiz., 2, 450, (1959).
3. R. H. Pantell, Proc. IRE, 47, 1146, (1959).
4. J. Schneider, Phys. Rev. Lett. 2, 504 (1959).
5. J. L. Hirshfield and J. M. Wachtel, Phys. Rev. Lett. 12, 533 (1964).
6. J. L. Hirshfield, I. B. Bernstein and J. M. Wachtel, IEEE J. QE-1, 237 (1965).
7. A. V. Gaponov, M. I. Petelin and V. K. Yulpalov, Radio Phys. Quantum Electron. 10, 794 (1967).
8. D. V. Kisel', G. S. Korablev, V. G. Navel'yev, M. I. Petelin and Sh. E. Tsimring, Radio Eng. Electron. Phys. 19, #4, 95 (1974).
9. N. I. Zaytsev, T. B. Pankratova, M. I. Petelin and V. A. Flyagin, Radio Eng. Electron. Phys. 19, #5, 103 (1974).
10. V. L. Granatstein, P. Sprangle, R. K. Parker and M. Herndon, J. Appl. Phys. 46, 2021 (1975).
11. E. Ott and W. M. Manheimer, IEEE Trans. PS-3, 1 (1975).
12. J. L. Hirshfield and V. L. Granatstein, IEEE Trans. MTT-25, 522 (1977).
13. P. Sprangle and W. M. Manheimer, Phys. Fluids, 18, 224 (1975).
14. P. Sprangle and A. T. Drobot, IEEE Trans. MTT-25, 528 (1977).
15. K. R. Chu and J. L. Hirshfield, Phys. Fluids, 21, 461, (1978).
16. P. Sprangle and R. A. Smith, J. Appl. Phys., 51, 3001, (1980).
17. M. E. Read, K. R. Chu and A. J. Dudas, NRL Memo Report No. 4169 (1981). AD-A 094 351
18. P. Sprangle, J. L. Vomvoridis and W. M. Manheimer, Appl. Phys. Lett., 38, 310, (1981), also Phys. Rev. A23, 3127, (1981).
19. I. E. Botvinnik, V. L. Bratman, A. B. Volkov, N. S. Ginzburg, G. G. Denisov, B. D. Kol'chugin, M. N. Ofitserov and M. I. Petelin, JETP Lett., Vol. 35, No. 10, pp. 516, (1982).
20. J. L. Vomvoridis and P. Sprangle Phys. Rev. A, 25, 931, (1982).
21. Y. Y. Lau, IEEE Trans., Vol. ED-29, No. 2, pp. 320, (1982).
22. V. L. Bratman, G. G. Denisov, N. S. Ginzburg and M. I. Petelin, IEEE J. Quantum Electron, Vol. QE-19, p. 282, (1983).

23. D. S. Birkett and T. C. Marshall, Phys. Fluids 24, 178 (1981).
24. A. T. Lin, W. W. Chang and C.-C. Lin, Phys. Fluids 27, 11054 (1984).
25. V. L. Bratman, M. A. Moiseev, M. I. Petelin and R. E. Erm, Radio Phys. Quantum Electron. 16, 474 (1973).
26. V. L. Granatstein, M. Herndon, R. K. Parker and P. Sprangle, IEEE J. Quantum Electron. QE-10 p. 651 (1974).
27. K. E. Kreischer and R. J. Temkin, Intl. J. of Infrared and Millimeter Waves, Vol. 2, No. 2, p. 175 (1981).
28. P. Drossart, H. Bohmer, J. M. Buzzi, H. J. Doucet, B. Etlicher, P. Haldenwang, H. Lamain and C. Rouille, Proc. 3rd Intl. Conf. on High Power Electron and Ion Beams, Novosibirsk, USSR (1979).
29. C. S. Wu and L. C. Lee, Ap. J. 230, 621 (1979).
30. H. P. Freund, H. K. Wong, C. S. Wu and M. J. Xu, Phys. Fluids 26, 2263 (1983).
31. C. S. Wu and H. P. Freund, Radio Sci. 19, 519 (1984).
32. R. R. Sharma, L. Vlahos and K. Papadopoulos, Astr. Ap. 112, 377 (1982).
33. D. B. Melrose and G. A. Dulk, Ap. J. 259, 844 (1982).
34. L. Vlahos and P. Sprangle, Univ. of Md. Memo Report No. AP85-039, also submitted to Ap. J. (1984).
35. Y. Y. Lau and K. R. Chu, Phys. Rev. Lett., 50, 243, (1983).
36. K. T. Tsang, Phys. Fluids 27, 1659 (1984).
37. A. A. Kolomenskii and A. N. Lebedev, Dok. Akad. Nauk. SSSR 145, 1259 (1962) and Sov. Phys. Dokl. 7, 745 (1963).
38. J. L. Vomvoridis, IEEE Trans. Nucl. Sci., 28, 3418, (1981).
39. P. Sprangle, L. Vlahos and C. M. Tang, IEEE Trans. Nucl. Sci. NS-30, 3177 (1983).
40. P. Sprangle and L. Vlahos, Ap. J. (Letters) 273, L95 (1983).
41. V. L. Bratman, N. S. Ginzburg and M. I. Petelin, Optics Commun. 30, 409 (1979).

END

FILMED

10-85

DTIC